Super-resolution and the radar point spread function*

R O Lane
rlane1@QinetiQ.com
QinetiQ Malvern

Abstract: The effect of residual uncompensated cross-track platform acceleration on the point spread function (PSF) of a synthetic-aperture radar (SAR) system is derived. This is compared to an approximate PSF model originally derived from an optics based argument, which previously has been proposed to be used for the super-resolution of SAR imagery. The PSFs are used in a comparison of three super-resolution algorithms based on a distributed scatterer model. It is shown that assuming no cross-track acceleration is present is better than using the optics approximation and knowledge of the correct cross-track acceleration gives the best performance.

1 Introduction

Super-resolution techniques attempt to increase the resolution of an imaging system beyond the theoretical physical limit through the use of signal processing and some form of prior knowledge about the scene and the imaging point spread function (PSF). A feature of super-resolution techniques is that the PSF must accurately be known for the results to be reliable. Synthetic-aperture radar (SAR) systems – used for a variety of purposes including day and night all-weather target recognition, terrain classification and remote sensing – coherently combine successive radar pulses to obtain high-resolution two-dimensional imagery. In SAR systems the precise PSF is dependent on the relative motion between the radar and the target so accurate knowledge of this motion is required before super-resolution can be performed. Although motion compensation and autofocus techniques attempt to remove the effects of unknown aircraft motion some residual errors may remain.

Blacknell performed a study [1] into the effects of using a stochastic description for the PSF based on a simulation of an airborne SAR system. The results showed that there was no advantage to using the stochastic description over a standard PSF model. These results were compared to another super-resolution study [2] that used a parametric model for the PSF based on an optics argument. It was not possible to make a conclusive judgment as to which technique is better due to the difference in the models used for simulation. The purpose of this paper is to derive an appropriate parametric model for the PSF based on radar physics, compare this with the optics-based PSF and determine if the two studies can be related more closely. Three super-resolution algorithms are compared using the two PSFs and the effect of a perturbed PSF is measured in terms of the physically meaningful parameter of cross-track acceleration. This is an improvement over previous work [3] where a simple Gaussian PSF was used.

The rest of the paper is organised as follows. Section 2 derives the PSF of a radar undergoing uniform motion and also when residual cross-track acceleration is present after focussing techniques. This is compared to the PSF derived from an optics based model that has previously been proposed to be used for the super-resolution of SAR imagery. Section 3 introduces three super-resolution algorithms and shows results of these algorithms using the PSFs derived earlier. Conclusions are drawn in section 4.

2 Point spread functions

2.1 Radar based PSF

The precise nature of the radar PSF is dependent on several aircraft and radar parameters. Where necessary, reasonable values for the parameters have been assumed and correspond to those used in the work of Oliver [4], on which this derivation is based. The relevant parameters are: minimum range R_0 = 40 km, wavelength λ = 0.03 m, antenna length d = 2 m, aircraft velocity v_x = 200 ms^{-1} and synthetic-aperture time T = 3 s.

For a sideways looking radar undergoing constant cross-track acceleration a_y the variation in phase with time is

$$\phi(t) = \frac{4\pi\Delta R}{\lambda} = (\beta_0 + \delta\beta)t^2, \tag{1}$$

where $\beta_0 = \frac{2\pi v_x^2}{R_0\lambda}$ and $\delta\beta = \frac{2\pi a_y}{\lambda}$. The signal received by the radar for a point target is $s(t) = \exp(-i\phi(t))$ and

*Appears in *Proceedings of the London Communications Symposium 2005*

the matched filter output is given by the cross-correlation of this with a reference signal $h^*(t) = \exp(i\beta_0 t^2)$:

$$g(t) = \frac{1}{T}\int_{-T/2}^{T/2} s(t+\tau)h^*(\tau)d\tau \quad (2)$$

$$= \frac{1}{T}\int_{-T/2}^{T/2} \exp\left[-i(\beta_0+\delta\beta)(t+\tau)^2 + i\beta_0\tau^2\right]d\tau \quad (3)$$

$$= \frac{1}{T}\exp\left[-i(\beta_0+\delta\beta)t^2\right]\int_{-T/2}^{T/2}\exp\left[-i(\beta_0+\delta\beta)2t\tau - i\delta\beta\tau^2\right]d\tau. \quad (4)$$

For zero cross-track acceleration $\delta\beta$=0 and this simplifies to the familiar sinc function $g(t) = \mathrm{sinc}(\beta_0 T t)\times \exp(-i\beta_0 t^2)$. When the cross-track acceleration is non-zero the integral in (4) can be Fourier transformed to give

$$I(\omega) = \frac{1}{T}\int_{-T/2}^{T/2}\exp\left(-i\delta\beta\tau^2\right)\int_{-T/2}^{T/2}\exp\left[-i(\beta_0+\delta\beta)2t\tau\right]\exp(i\omega t)dtd\tau \quad (5)$$

$$= \int_{-T/2}^{T/2}\exp\left(-i\delta\beta\tau^2\right)\mathrm{sinc}\left(\left[(\beta_0+\delta\beta)2\tau-\omega\right]\frac{T}{2}\right)d\tau. \quad (6)$$

If $\frac{\pi}{(\beta_0+\delta\beta)T} \ll \frac{T}{2}$, which holds well for the parameters used here, then the sinc function may be approximated by an expression proportional to the Dirac delta function $\delta\left(\tau - \frac{\omega}{2(\beta_0+\delta\beta)}\right)$ and

$$I(\omega) \propto \exp\left[\frac{-i\delta\beta\omega^2}{4(\beta_0+\delta\beta)^2}\right]. \quad (7)$$

The inverse Fourier transform of this function cannot be evaluated in terms of simple functions. However, the analytical form when using integration limits $\omega = \pm W/2$ is given by Mathematica 4.0 [5] as

$$I(t) \propto \frac{\sqrt{\pi}(-1)^{1/4}(\beta_0+\delta\beta)}{W\sqrt{\delta\beta}}\exp\left[\frac{i(\beta_0+\delta\beta)^2t^2}{\delta\beta}\right]\times ... \quad (8)$$
$$\left\{\mathrm{erfi}\left[\frac{(-1)^{3/4}\left[4(\beta_0+\delta\beta)^2t-\delta\beta W\right]}{4\sqrt{\delta\beta}(\beta_0+\delta\beta)}\right] - \mathrm{erfi}\left[\frac{(-1)^{3/4}\left[4(\beta_0+\delta\beta)^2t+\delta\beta W\right]}{4\sqrt{\delta\beta}(\beta_0+\delta\beta)}\right]\right\},$$

where $\mathrm{erfi}(z) = \mathrm{erf}(iz)/i$ and $\mathrm{erf}(z) = (2/\sqrt{\pi})\int_0^z \exp(-t^2)dt$. This can be substituted for the integral in (4) to give the desired PSF as a function of time. To obtain the PSF in spatial co-ordinates t is replaced with x/v_x.

2.2 Optics based PSF

In the paper by Luttrell [2] it is stated that a SAR system undergoing anomalous motion can in first order be modelled as the defocussing of a simple linear imaging system. The point spread function is given as

$$g(x) = \frac{1}{2c}\int_{-c}^{+c}\exp(ikx + i\theta k^2x^2)dk. \quad (9)$$

The paper goes on to make a linear approximation valid when $|\theta c^2x^2| \lesssim 1$ to solve this analytically. It is stated that for super-resolution within the main lobe $|x| < \pi/c$ and it is required that $|\theta| \lesssim 0.1$. However, it should be noted that in practice the image obtained from a radar will also contain energy in the side-lobes and either a much smaller value of θ should be used, which would limit the range of motion that can be accomodated, or the approximation would have to be be expanded to quadratic or higher orders of θ. If the approximation were expanded then Luttrell's autofocus/super-resolution algorithm would no longer apply because it depends on a PSF linear in θ. It is in fact possible to evaluate the integral (9) in terms of special functions and is given by Mathematica as:

$$g(x) = \frac{(-1)^{3/4}e^{-i/(4\theta)}\sqrt{\pi}}{4c\sqrt{\theta}x}\left[\mathrm{erfi}\left(\frac{(-1)^{1/4}(1-2c\theta x)}{2\sqrt{\theta}}\right) - \mathrm{erfi}\left(\frac{(-1)^{1/4}(1+2c\theta x)}{2\sqrt{\theta}}\right)\right]. \quad (10)$$

2.3 PSF comparison

A comparison between the optics model and the radar cross-track acceleration model was made by setting integration limits such that the -3dB resolution with no distortion was 1m for both models, setting θ to various values

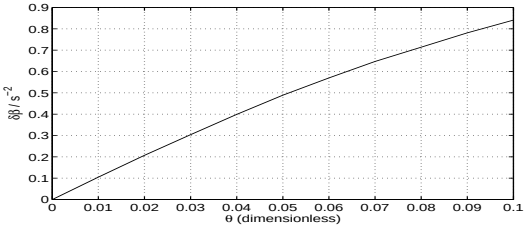

Figure 1: Relationship between defocus parameters

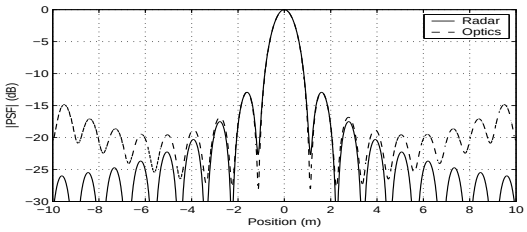

(a) $\theta = 0.02$, $\delta\beta = 0.207s^{-2}$

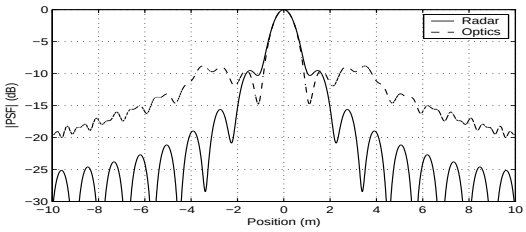

(b) $\theta = 0.10$, $\delta\beta = 0.831s^{-2}$

Figure 2: Comparison of radar and optics PSFs for two levels of defocus

and then adjusting $\delta\beta$ until the two PSFs had the same first side-lobe level. The corresponding values of θ and $\delta\beta$ are displayed in Figure 1 showing a mildly non-linear relationship between the two defocus parameters. From the graph and using the assumed radar parameters, the residual cross-track acceleration corresponding to θ=0.1 (the value used in [2], [6], [7] and [8]) is 4.0×10^{-3} ms^{-2}.

Examples of the PSFs are shown in Figures 2a and 2b where θ=0.02 and 0.10 respectively. For θ=0.02 the level of defocus is low and the two PSFs are similar both to each other and to a completely focussed sinc function (not shown) for the first few side-lobes. However, at larger distances from the main lobe the PSFs start to diverge with the optics PSF showing more distortion. For θ=0.10 the PSFs are substantially different. The optics PSF has a much higher level of distortion and the first side-lobe is no longer the strongest. In comparison, the radar cross-track acceleration PSF has deteriorated only slightly and is still similar to a sinc function. The resolution of the two PSFs degraded by about 3.6% for $\theta = 0.10$ and 5.0% for $\delta\beta = 0.831s^{-2}$.

3 Super-resolution results

Three standard super-resolution algorithms are tested here: inverse (INV), singular value decomposition (SVD) and thresholded minimum mean square error (MMSE-T). An overview of these algorithms and others including Bayesian super-resolution [6] is given in [8]. A super-resolution performance metric is the output signal-to-noise ratio defined as $SNR_{out} = ||f||^2/||\hat{f} - f||^2$, where f is the true high-resolution scene and $\hat{f}$ is the estimated scene using any particular algorithm. A Monte Carlo assessment has been carried out using measured SAR data. A high-resolution target image of 27x33 pixels had its resolution degraded using the cross-track acceleration PSF with $\delta\beta = 0.831s^{-2}$ and noise was added at an SNR of 30dB. Each super-resolution algorithm was then executed using the correct cross-track acceleration PSF, the optical PSF with the correct first side-lobe level ($\theta = 0.10$), and a sinc PSF. This was repeated 100 times and the mean and standard deviations of the output SNR were measured.

Results of the assessment are shown in Table 1. The radar PSF gives the best performance for SVD and MMSE-T, which are the most reliable algorithms. This is to be expected as cross-track acceleration is the correct model used in the simulation. Using the optics PSF gives a worse performance than using a sinc function. This is because the optics PSF is less similar to the sinc function than the radar PSF. Example imagery before and after super-resolution using MMSE-T and the radar PSF is shown in Figure 3.

4 Conclusions

A radar and optics PSF have been compared using analytic expressions for the functions. The effect of using the optics PSF during super-resolution when the actual PSF is due to cross-track acceleration was found to be worse than using an idealised sinc function when no cross-track acceleration is present. Out of the algorithms tested MMSE-T was the best using the output SNR metric, which confirms previous results [8]. The best super-resolution

Algorithm	Radar PSF		Optics PSF		Sinc PSF	
	Mean	S.D.	Mean	S.D.	Mean	S.D.
INV	-11.83	1.16	-1.46	0.31	-4.16	1.10
SVD	8.85	0.08	2.14	0.03	8.10	0.11
MMSE-T	10.52	0.44	2.22	0.10	8.19	1.40

Table 1: Output SNR in dB

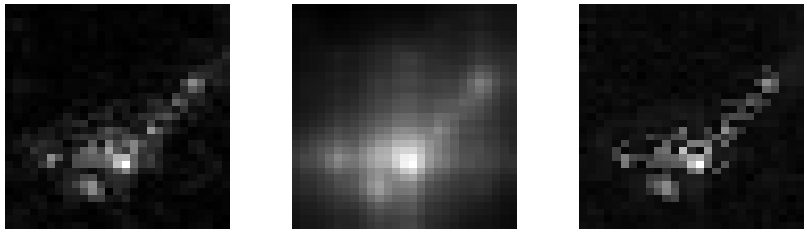

Figure 3: Original, blurred and super-resolved images

metric for an automatic target recognition (ATR) application would be overall classification performance, which has been used in [7] and [9].

Finally it should be noted that effects other than anomalous motion between the radar and target may alter the PSF. Phase noise or non-linearities due to imperfections of the radar receiver, quantisation noise and atmospheric phase disturbances all increase side-lobe levels. Also, scattering centres whose properties vary with frequency and imaging geometry result in non-ideal PSFs. These effects would further reduce the performance of standard super-resolution algorithms.

Acknowledgments

This work was sponsored by the EPSRC Engineering Doctorate programme and the UK Ministry of Defence Corporate Research Programme.

References

[1] D. Blacknell and S. Quegan, "SAR super-resolution using a perturbed point spread function," *IGARSS*, pp. 2592–2595, July 1989.

[2] S. P. Luttrell, "A Bayesian derivation of an iterative autofocus/superresolution algorithm," *Inverse Problems* **6**(6), pp. 975–996, 1990.

[3] R. O. Lane, "Estimating radar cross section using Bayesian image restoration," *Proceedings of the London Communications Symposium*, pp. 1–4, September 2003.

[4] C. J. Oliver, "Synthetic-aperture radar imaging," *J. Phys. D: Appl. Phys.* **22**, pp. 871–890, 1989.

[5] S. Wolfram, *The Mathematica Book*, Wolfram Media/CUP, 4th ed., 1999.

[6] R. O. Lane, K. D. Copsey, and A. R. Webb, "A Bayesian approach to simultaneous autofocus and super-resolution," *Proc. of SPIE vol. 5427, Algorithms for synthetic aperture radar imagery XI*, pp. 133–142, April 2004.

[7] K. D. Copsey, R. O. Lane, and A. R. Webb, "Designing NCTR algorithms when operating sensor conditions differ from training conditions," *International conference on radar systems (Radar2004), Toulouse, France*, October 2004.

[8] R. O. Lane, K. D. Copsey, and A. R. Webb, "Assessment of a Bayesian approach to recognising relocatable targets," *NATO RTO SET-096 specialists' meeting on the millimeterwave advanced target recognition and identification experiment (MATRIX 2005), Oberammergau, Germany*, May 2005.

[9] L. M. Novak, G. J. Owirka, and A. L. Weaver, "Automatic target recognition using enhanced resolution SAR data," *IEEE Transactions on Aerospace and Electronic Systems* **35**, pp. 157–175, January 1999.